PHYSICAL REVIEW A VOLUME 22, NUMBER 3 SEPTEMBER 1980

Experimental and theoretical investigation of the optogalvanic effect in the helium positive column

James E. Lawler
Department of Physics, Stanford University, Stanford, California 94305
(Received 9 October 1979; revised manuscript received 31 March 1980)

A linear, steady-state analytical model of the optogalvanic effect in a positive column on the 587.6-nm He transition is presented. Absolute measurements of the optogalvanic effect in a positive column on the 587.6-nm He transition are reported. The model and the experiment are found to agree over a substantial range of direct currents and over a factor of 10 in column-radius–pressure product. This model relates the absolute magnitude of the optogalvanic effect on one transition to a known ionization rate. The structure of this model should be useful in determining ionization rates of electronically excited levels from optogalvanic measurements.

I. INTRODUCTION

The optogalvanic effect, reported in positive column and hollow cathode discharges,[1] is used as a sensitive detection method in laser spectroscopy. Although the optogalvanic effect was first observed over 50 years ago (see Ref. 2 for a review of early work), the potential of the phenomena as a detection method has been widely recognized only recently. Trace element detection at the 0.1 ppb level is possible with optogalvanic detection.[3] High-resolution spectroscopy on single-photon transitions is performed using Doppler-free intermodulated optogalvanic spectroscopy.[4] Doppler-free two-photon transitions are also studied using optogalvanic detection.[5]

There is need for an improved theoretical understanding of the optogalvanic effect. An improved theoretical understanding of the effect might lead to improvements in the sensitivity of optogalvanic detection in trace element analysis and in high-resolution Doppler-free spectroscopy. The work of Smyth, Keller, and Crim,[6] Pepper,[7] and Zalewski, Keller, and Engleman,[8,9] are significant steps in this direction.

Besides the hope of improvement in the sensitivity of optogalvanic detection, there are other motivations for this work. The magnitude of the optogalvanic effect is dependent on the magnitude of the ionization rates of levels whose populations are perturbed by the laser. The model described in this paper successfully relates, for one transition, the absolute magnitude of the optogalvanic effect to a known ionization rate. It should be possible to study other transitions and use the absolute magnitude of the optogalvanic effect to determine ionization rates of electronically excited levels.

The positive column discharge is not in local thermodynamic equilibrium and is therefore best described by rate equations. A perturbation to the column, such as the optogalvanic effect, must also be described by rate equations.[7] Unfortunately, one rarely knows a sufficient number of cross sections to completely solve the problem. This paper describes a new approach to a rate-equation description of the optogalvanic effect. The rate-equation problem is split into two parts. The first part involves solving the rate equations exactly for a few levels whose populations are greatly perturbed by the laser. The solution is expressed as an ionization efficiency, the number of excess ion-electron pairs produced per absorbed photon. The second part of the problem involves describing the electrical response of the plasma to a small perturbation in the total ion production rate. The second part of the problem is solved by a linear, steady-state perturbation analysis of the key rate equation or equations which describe the plasma. The solution can be expressed as a collection efficiency, the number of excess electrons which flow through the ballast resistor per excess ion-electron pair produced in the plasma. The dynamic resistance of the column plays an important role in the linear analysis of the key rate equation(s). The dynamic resistance is difficult to calculate from first principles but is trivial to measure. Each transition has a unique ionization efficiency, but the collection efficiency is a property of the plasma. The quantum efficiency of the optogalvanic effect is the product of the ionization efficiency and the collection efficiency.

The model is tested by studying a single He transition involving only levels with well understood kinetics and well known reaction rates. Measurements of the absolute magnitude of the optogalvanic effect per absorbed photon are reported over a range of experimental parameters. The experimental parameters which are varied

include the laser intensity, column radius, column pressure, direct current in the column, and ballast resistor. The model agrees with the current dependence of the optogalvanic effect and the absolute magnitude of the effect over a wide range of Rp (the product of column radius and column pressure).

II. He KINETICS AND THE IONIZATION EFFICIENCY

The choice of a transition involving only levels with well understood kinetics for this study is essential. The He discharge is one of the most thoroughly studied discharge systems (for example, see Ref. 10 and extensive bibliography), and He radiative decay rates are also very accurately known.[11] The He 2^3P-3^3D transition is ideal because of its convenient wavelength 587.6 nm, and because most of the kinetics of the 3^3D level,[12-15] the 2^3P level,[16] and other nearby levels[12-18] are known. Although electron-impact ionization cross sections for the 2^3P and 3^3D levels have not been measured they can be neglected. The electron density in this study is typically 2×10^{11} cm^{-3} or less, and the average electron thermal velocity is approximately 2×10^{8} cm/sec or less. Electron-impact ionization is neglected because the cross section must be 10^{-13} cm^2 or more before the resultant rate is comparable to the associative ionization rate of the 3^3D. Reasonable estimates, based on hydrogen calculations, of the electron-impact ionization cross section of the 2^3P and 3^3D levels are less than or equal to 10^{-14} cm^2.[18] The rates of important radiative and collisional decay channels of the 3^3D and 2^3P levels are summarized in Fig. 1.[11-13]

The ionization efficiency of the 2^3P-3^3D transition can be determined by inspection of Fig. 1. It is apparent from Fig. 1 that the dominant decay channel of an atom in the 3^3D level is spontaneous decay at 587.6 nm. It is also apparent that the dominant channel producing an ion-electron pair is associative ionization. Associative ionization refers to the production of a He molecular ion and a free electron by a two-body collision between a ground-state He atom and an excited He atom in a state above the 3s levels. Suppose that a dye laser irradiating the discharge is tuned to 587.6 nm; some He atoms in the 2^3P level absorb laser photons and are elevated to the 3^3D level. If the laser intensity is far below saturation it is apparent that the efficiency of ionization per absorbed photon is approximately the ratio of the associative ionization rate a to the spontaneous radiative decay rate A. Net absorption of a photon is measured by the attenuation of the laser beam, hence the efficiency of ionization is unchanged as the laser intensity is increased

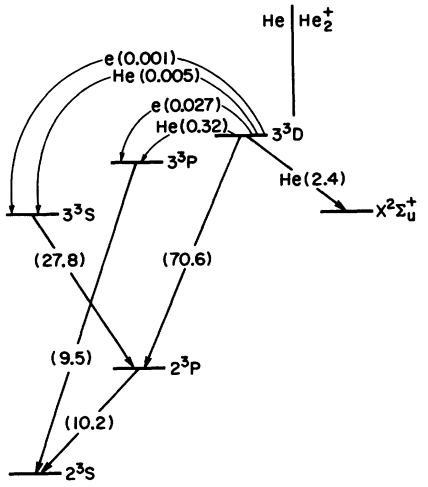

FIG. 1. Summary of spontaneous radiative rates and collisional rates of reactions involving the 3^3D level. The numbers enclosed in parentheses are rates in units of 10^6 sec^{-1}. Collisional processes are indicated by a symbol for the collision partner preceding the rate. The collisional rates are for a discharge with 1.0 Torr of He, with an electron concentration of 1.7×10^{11} cm^{-3}, and with an electron temperature of 6.5 eV.

to the saturation intensity or higher. If an atom absorbs a photon and is subsequently stimulated by the laser beam to emit radiation, no attenuation of the laser beam is detected. The ionization efficiency a/A is 0.033 at 1.0 Torr. By modeling and measuring the optogalvanic response per absorbed photon it is possible to avoid any calculation or measurement of the production rate of He atoms in the 2^3P level.

The expression for the ionization efficiency is particularly simple in the case of the 2^3P-3^3D transition. In a more general case described in the Appendix the ionization efficiency is determined by a set of coupled rate equations. Other ionizing reactions could be important for other levels. If electron-impact ionization is important, the electron density and temperature must be measured to relate the ionization efficiency to an ionization cross section. If metastable collisions are important, the metastable density must be measured to relate the ionization efficiency to an ionization cross section. Time-resolved spectroscopic measurementsof total decay rates and collisional transfer rates will usually be necessary.[12-17] Nevertheless, the optogalvanic effect should be useful in kinetics studies because it provides a convenient and sensitive means of measuring small perturbations to the ion density.

It should be noted that the ionization efficiency can be negative as well as positive.[6] A negative optogalvanic effect is observed in Ne when the

metastable population is depleted by pumping a level which can radiate to the ground state. The metastable population limits ion production through two-step electron-impact ionization. The overall efficiency of the optogalvanic effect in this case is often comparable to the efficiency when fast associative ionization or chemionization channels are open.

III. THE COLLECTION EFFICIENCY

The collection efficiency is determined by a linear, steady-state perturbation analysis of the most important rate equation(s) which describe the plasma. The single most important rate equation is the rate equation for ions. The ion rate equation plays a key role in very early positive column models,[19] as well as very recent work.[20]

It is assumed that the magnitude of the optogalvanic effect is linear per absorbed photon. This assumption is reasonable because the laser produces at most a few percent change in the discharge current. Substantial experimental data support this assumption, the optogalvanic effect on the 2^3P-3^3D transition saturates with the absorption as the laser power is increased. The model will not treat the dependence of the optogalvanic effect on the spatial distribution of absorbed photons. The optogalvanic response per absorbed photon is observed to be 10 to 20% larger when the laser is focused on the column axis than it is when the laser uniformly illuminates the column. This spatially averaged model is a good approximation.

In the following discussion the electron concentration on axis n and the axial electric field E are treated as independent variables. The column radius R and the pressure p are fixed parameters. Most models of the positive column can be cast in a mathematical framework which involves two key equations: the ion rate equation

$$G(n,E)=0=\frac{dN}{dt}, \tag{1}$$

and the direct current equation

$$i=F(n,E). \tag{2}$$

The function G is composed of an ion production term minus an ion loss term in units of ions per sec and N is the total number of ions in the plasma. Both terms are dependent on the electron concentration n and E/p. The sustaining direct current i is determined by the external circuit; hence Eqs. (1) and (2) determine n and E during steady-state operation. This is a convenient framework because n and E/p are two parameters which completely characterize a discharge. Explicit expressions for G and F are given in the next section.

The laser produces excess ion-electron pairs when it is tuned to the 587.6-nm He transition. The excess ion-electron pairs perturb n and E; hence

$$\frac{\partial G}{\partial n}\Delta n+\frac{\partial G}{\partial E}\Delta E+\frac{a}{A}Q=0=\frac{dN}{dt}, \tag{3}$$

where a/A is the previously defined ionization efficiency and Q is the total number of photons absorbed per unit time. The current is also perturbed; hence

$$\Delta i=\frac{\partial F}{\partial n}\Delta n+\frac{\partial F}{\partial E}\Delta E. \tag{4}$$

The external circuit provides the necessary additional constraint

$$Z\Delta i=-l\Delta E, \tag{5}$$

where Z is the ballast resistance plus the power supply impedance and l is the length of the column. If the cathode fall is not independent of current it is desirable to include in Z additional dynamic resistance due to the cathode fall. Equations (3), (4), and (5) are solved to yield

$$\Delta i=-\frac{a}{A}Q\frac{\partial F}{\partial n}\frac{l}{Z}\Big/\left[\frac{\partial G}{\partial n}\left(\frac{\partial F}{\partial E}+\frac{l}{Z}\right)-\frac{\partial G}{\partial E}\frac{\partial F}{\partial n}\right]. \tag{6}$$

It is desirable to simplify Eq. (6) by using Eqs. (1) and (2) to evaluate the total derivative of the direct current with respect to the electric field

$$\frac{di}{dE}=\frac{\partial F}{\partial E}-\frac{\partial F}{\partial n}\frac{\partial G}{\partial E}\Big/\frac{\partial G}{\partial n}. \tag{7}$$

This total derivative is closely related to the dynamic resistance of the column

$$\frac{dV}{di}=l\Big/\frac{di}{dE}, \tag{8}$$

where V is the column voltage. Equation (6) is simplified as

$$\Delta i=-\frac{a}{A}Q\left(\frac{\partial F}{\partial n}\Big/\frac{\partial G}{\partial n}\right)\frac{dV}{di}\Big/\left(\frac{dV}{di}+Z\right). \tag{9}$$

It is essential to note that no assumptions about the dominant ion production mechanism, the dominant ion loss mechanism, or the dominant metastable loss mechanism are necessary to derive Eq. (9). Much of the dependence of the optogalvanic response per absorbed photon on the sustaining direct current is due to the dynamic resistance of the column which is a strong function of current. The dynamic resistance of the column is an easily measured parameter which can be used to relate the optogalvanic response per absorbed photon to the kinetics

of the levels perturbed by the laser. Assumptions about the dominant mechanisms in the column are required to evaluate the remaining partial derivatives in Eq. (9).

The model of the optogalvanic effect described in this section is a very simple model and several improvements can be suggested. The metastable density could be introduced as an additional independent variable with an additional rate equation. This would be essential if the laser directly depleted the metastables by pumping a level which can radiate to the ground state. The atomic ion density and molecular ion density could be introduced as separate independent variables with separate rate equations. The introduction of additional independent variables with additional rate equations will not change the role played by the dynamic resistance. The role played by the dynamic resistance is determined by the assumption that the plasma responds linearly to the perturbation.

IV. THE POSITIVE COLUMN MODEL

The model of the He positive column used in this work is closely related to the Tonks and Langmuir[21] "free fall" model with modifications suggested by the work of Cherrington.[20] The essential features of the positive column model are the following:

(1) the Debye length is much less than the column radius,

(2) diffusion is the dominant metastable loss process,

(3) ion production is dominated by two-step electron impact ionization,

(4) ion loss is dominated by wall losses.

Assumption (1) implies that the electron and ion concentrations are essentially equal in the plasma. This assumption does not hold in the sheath, the boundary of the plasma. The axial electron concentration n will be used in place of the axial ion concentration.

Metastable He atoms play a key role in ion production. Assumption (2) implies that the metastable concentration is approximately linear with electron concentration and with sustaining direct current. This assumption constrains the model to low currents. At high currents the metastable population saturates due to destruction by electron collisions (superelastic and ionizing) and due to collisions between pairs of metastables. It is essential in the experiments to be compared with this model that data be collected at low currents where the metastable population is not saturated. There are a substantial number of studies of metastable populations as a function of current which can be used to define the desired range of currents as a function of Rp.[22-25] The metastable diffusion coefficient,[26] the metastable electron-impact ionization cross section,[27] the metastable electron-impact superelastic collision cross section,[10] and the metastable-metastable destruction cross section[28] are all well known. This information is also useful in defining the desired range of currents where the metastable population is proportional to the current.

Assumption (3) together with assumption (2) imply that the ion production rate is proportional to n^2. Several processes, which involve metastables, can be included in two-step electron-impact ionization. The rate of ion production due to direct electron-impact ionization of metastables, collisions between pairs of metastables, and indirect electron-impact ionization of metastables would all be proportional to n^2 if the metastable population is not saturated. Indirect electron-impact ionization of metastables includes electron-impact excitation of a metastable to a level which can associatively ionize or autoionize. The importance of two-step electron-impact ionization in the rare-gas positive column has been known for some time.[29] Recently Cherrington derived a very successful positive column scaling law using two-step ionization as the dominant ion production mechanism.[20]

Assumption (4), that wall losses dominate bulk recombination in the positive column, was recognized by Schottky. He described the process in terms of ambipolar diffusion.[19] Tonks and Langmuir presented a more general description of the ion motion to the wall. Their treatment applies for small values of Rp where the ion mean free path is larger than the column radius. Their treatment agrees with the Schottky model when the ion mean free path is smaller than the column radius. The data presented in this paper cover values of Rp from 0.05 to 0.5 cm Torr. The ion mean free path is smaller than the column radius over this range of Rp, and hence it would appear that ambipolar diffusion would best describe the ion wall current. This, however, is not the case. Bickerton and von Engel concluded that the ion wall current is best described by the Tonks and Langmuir free fall model in this range of Rp in the He positive column.[30] They based their conclusion on measurements of the electron temperature as a function of Rp. They reasoned that this is a consequence of the large radial electric field which results from the relatively high electron temperature always found in rare gases. This imparts to the ions a motion which is strongly directed towards the tube wall, so that their drift velocity is not a small fraction of

their random thermal velocity.[30] The Schottky model assumed that the ion motion is isothermal ion drift.

It is possible using assumption (1) through (4) to write more explicit expressions for F and G as defined in the previous section. The electron mobility is two orders of magnitude higher than the ion mobility, hence the sustaining direct current is carried by the electrons. The sustaining direct current is

$$i = F(n,E) = en\mu E\pi R^2 2h_0 , \tag{10}$$

where e is the electron charge, μ is the electron mobility, and h_0 is a constant defined by Tonks and Langmuir which relates the average and axial electron concentration.[21] The ion rate equation contains a production term proportional to n^2, and a loss term proportional to n which is the ion wall current. The ion rate equation is

$$G(n,E) = g(E)n^2 - n(2kT_e/m_p)^{1/2}2\pi Rls_0h_0$$
$$= 0 = \frac{dN}{dt} . \tag{11}$$

The function $g(E)$ contains electron-impact rates which are functions of E/p, the metastable diffusion coefficient, other collision rates, and fixed parameters like R and p. It will not be necessary to specify the exact form of $g(E)$. The parameter k is Boltzman's constant, T_e is the electron temperature, and m_p is the ion mass. The constant s_0, defined by Tonks and Langmuir, was calculated for positive columns with uniform production ($s_0 = 0.638$) and with ion production proportional to the electron density ($s_0 = 0.772$).[21] The value of s_0 for ion production with a spatial dependence described by the square of the lowest-order diffusion mode is calculated to be 1.0. The details of this calculation will not be presented; as an approximation, the value $s_0 = 0.77$ will be used in this work. Although a Maxwell-Boltzmann distribution for calculating electron- used in the derivation of the ion wall current, it should be emphasized that this model of the optogalvanic effect does not require a Maxwell-Boltzman distribution for calculating electron-impact excitation or ionization rates. The electron-impact rates and the parameter kT_e in the ion wall current are functions of E/p.

The remaining partial derivatives in Eq. (9) are now evaluated as

$$\frac{\partial F}{\partial n} \Big/ \frac{\partial G}{\partial n} = eR\mu E \Big/ s_0 l \left(\frac{2kT_e}{m_p}\right)^{1/2} . \tag{12}$$

This ratio is equal to the ratio of the sustaining direct current to the ion wall current.

The model of the positive column described in this section is a very simple model and several improvements can be suggested. The effect of ion-atom collisions in retarding the ion motion toward the wall could be included. Single-step electron-impact ionization could be included. The effects of gas heating in the positive column could be included. These improvements and the improvements suggested at the end of the preceding section are desirable but not necessary to model the optogalvanic effect on the 2^3P-3^3D transition.

V. EXPERIMENTAL

Two discharge tubes were used in this experimental investigation. Both tubes are pyrex with tungsten-uranium glass electrical feedthroughs; they are coupled to a diffusion pump station through a glass to metal transition and a packless high vacuum valve. The tubes are operated as sealed discharge tubes. The first tube has a common cathode with several columns of different radius and separate anodes. The cathode is a neon sign cathode. The second tube has a 0.25-cm column radius and a large concentric aluminum cathode from a He-Ne laser. The magnitude of the optogalvanic effect in the positive column was not influenced by the cathode design. Both tubes were cleaned by extensive baking and by repeatedly running a high-current He discharge followed by evacuation of the tube. Ultimate vacuums attained are less than or equal to 10^{-7} Torr. The appearance of clean He emission spectra coincides with a strong optogalvanic effect. Ultra-high-purity He (99.999%) is used in this work. All pressure measurements are performed with a capacitance manometer.

An actively stabilized single frequency dye laser is used in this work. The laser bandwidth (1 MHz) is a small fraction of the Doppler width (2 GHz). The laser beam is directed down the axis of the positive column, it illuminates the column almost uniformly. All laser power and absorption measurements are performed with a calibrated thermopile. Measurements of the change in current caused by the laser are performed by monitoring the voltage across part of the ballast resitor with a calibrated lock-in amplifier.

The analytical model of the optogalvanic effect described in this paper is a steady-state model. In the experimental work the laser is chopped at a sufficiently low frequency (90 Hz) to ensure that a steady-state discharge is established during a small fraction of the on and off period of the chopping cycle. It is straightforward to test this assumption experimentally.

The dynamic resistance of the column was

measured at frequencies above and below the laser chopping frequency of 90 Hz. A very-low-frequency measurement of the dynamic resistance is performed with two digital voltmeters. One digital voltmeter is used to measure the discharge tube voltage and the second is used to measure the ballast resistor voltage while the power supply voltage is varied by hand. A second-120-Hz measurement is performed using the power supply ripple voltage and two oscilloscopes to measure the ripple voltage on the tube and ballast resistor. The dynamic resistance measurements at very-low-frequency and at 120 H_z are in agreement. Additional low-frequency measurements are made with plasma probes at each end of the column, these measurements confirmed that the cathode fall is current independent. The large negative dynamic resistance of the discharge tube is due to the positive column. Axial electric-field measurements are made with plasma probes at each end of the column.

VI. COMPARISON OF EXPERIMENT AND MODEL

The model of the optogalvanic effect described in the preceding sections predicts that the signal current is given as

$$\Delta i = -\frac{a}{A}Q\left[eR\mu E/0.77l\left(\frac{2kT_e}{m_p}\right)^{1/2}\right] \times \frac{dV}{di}\Big/\left(\frac{dV}{di}+Z\right). \tag{13}$$

Experimental measurements of the dynamic resistance of the column dV/di are presented in Figs. 2(a) through 6(a) as plots of $-dV/di$ versus i for fixed R and fixed p. Experimental measurements of the magnitude of the optogalvanic effect are presented in Figs. 2(b) through 6(b) as plots of the quantum efficiency $\Delta i/(eQ)$ versus $-(dV/di)/(dV/di+Z)$. The quantum efficiency is measured over a range of sustaining direct current at fixed ballast resistance and over a range of ballast resistance at fixed sustaining direct current. The measurements of the optogalvanic response are usually reproducible to 15%, even using different discharge tubes with the same column radius, pressure, and sustaining direct current.

The model predicts that data points for the optogalvanic effect should lie on a line which intercepts the origin and which has a slope of $(a/A)R\mu E/0.77l(2KT_e/m_p)^{1/2}$. The predictions of the model are presented as solid lines on the data plots. In the model predictions, the associative ionization rate a is $2.4\times10^6\times p$ sec^{-1} (where p is in Torr)[13]; the Einstein A is 7.06×10^7 sec^{-1} (Ref. 11); the electron mobility μ is $7.5\times10^5/p$ $\text{cm}^2/(\text{volt sec})$ (again p is in Torr)[31]; and l is 13.5 cm. Measurements of the axial electric field E for each value of Rp are used. The electron temperature T_e for each value of Rp is taken from Bickerton and von Engel.[30] Both E/p and kT_e are weakly dependent on current and strongly dependent on Rp. The weak and (similar) current dependences are ignored. The ion mass m_p is taken as the mass of the He molecular ion because molecular ions are produced in the associative ionization process which perturbs the discharge. This step is justified by introducing the atomic ion

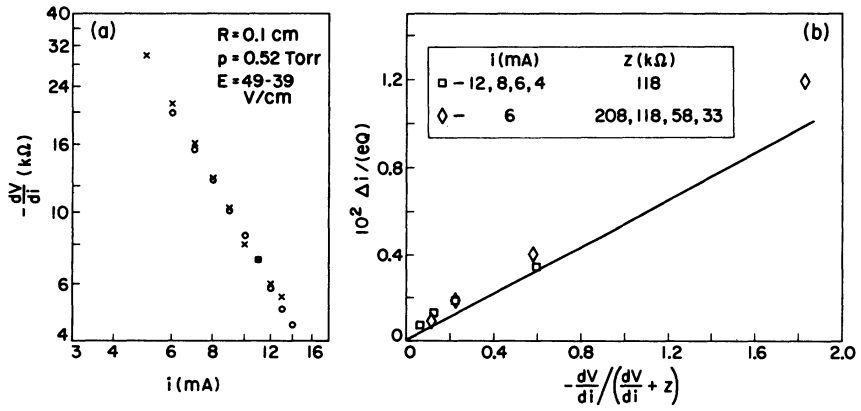

FIG. 2. (a) Dynamic resistance measurements at very low frequency for an Rp of 0.05 cm Torr. The symbol x represents a measurement across the entire discharge tube. The symbol O represents a measurement across only the positive column. (b) Measurements of the magnitude of the optogalvanic effect for an Rp of 0.05 cm Torr. The vertical axis can also be read as a quantum efficiency in %. The square symbols represent measurements over a range of sustaining direct current with a fixed ballast resistance. These measurements start at high current in the lower left corner of the plot. The diamond symbols represent measurements over a range of ballast resistance with a fixed sustaining direct current. These measurements start at high ballast resistance in the lower left corner of the plot. The solid line represents the prediction of the model. The estimated accuracy of the model is ±25%.

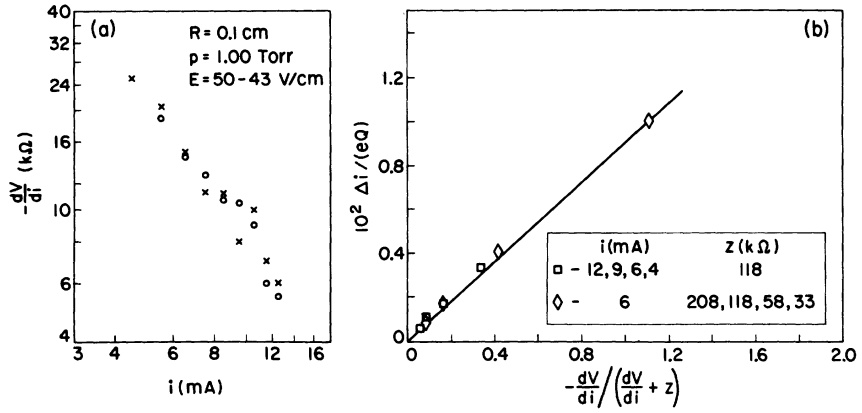

FIG. 3. Dynamic resistance measurements at very low frequency for an Rp of 0.10 cm Torr. (b) Measurements of the magnitude of the optogalvanic effect for an Rp of 0.10 cm Torr.

density and molecular ion density as separate independent variables with separate rate equations. The details of this simple calculation are omitted.

There are a number of simplifying assumptions in the derivation of Eq. (13). These assumptions lead one to expect that Eq. (13) should agree with the data to 25% at best. There are also uncertainties associated with each measured parameter in Eq. (13). The associative ionization rate has an uncertainty of 11%,[13] the electron mobility has an uncertainty of at least 10%,[31] and the electron temperatures have uncertainties of at least 10%. There are errors ($\leq 20\%$) associated with the fact that the electron temperature measurements and the optogalvanic measurements were not made under identical conditions. The agreement of the model with the current dependence and with the absolute magnitude of the optogalvanic effect is satisfactory over a factor of 10 in Rp. Attempts to fit the data using Schottky's expression for the ion wall current (ambipolar diffusion) result in satisfactory agreement over a much smaller range of Rp, 0.20–0.25 cm Torr. Agreement of the model and the experiment on the current dependence of the optogalvanic effect supports the hypothesis that associative ionization of the 3^3D is the dominant process producing the effect rather than electron impact ionization of the 3^3D or 2^3P levels.

The quantum efficiency of the optogalvanic effect on the 587.6-nm He transition is observed to be relatively insensitive to pressure. This occurs because the pressure dependence of the associative ionization rate cancels the pressure dependence of the electron mobility. This observation has important implications for Doppler-free optogalvanic spectroscopy. It is essential to perform Doppler-free spectroscopy at a small fraction of a Torr to minimize pressure broadening.

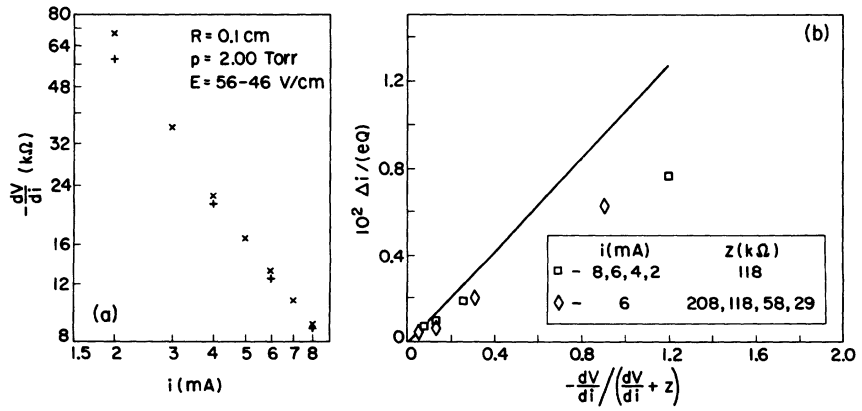

FIG. 4. Dynamic resistance measurements for an Rp of 0.20 cm Torr. The symbol × represents a measurement at very low frequency; the symbol + represents a measurement at 120 Hz. (b) Measurements of the magnitude of the optogalvanic effect for an Rp of 0.20 cm Torr.

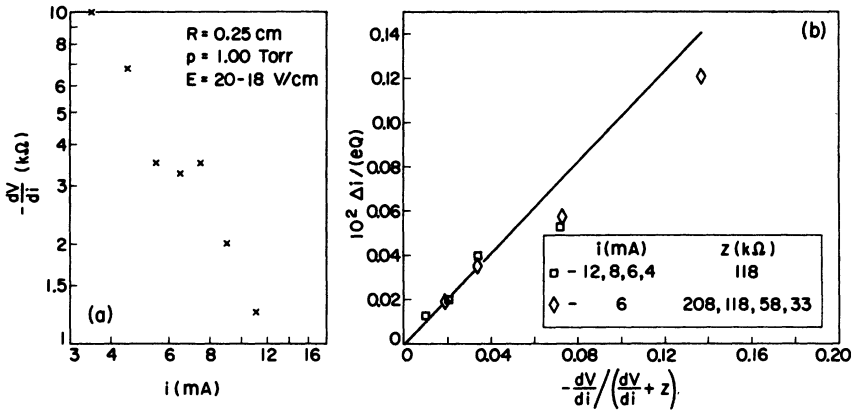

FIG. 5. (a) Dynamic resistance measurements for an Rp of 0.25 cm Torr. (b) Measurements of the magnitude of the optogalvanic effect for an Rp of 0.25 cm Torr.

VII. CONCLUSION

A linear, steady-state, analytical model on the optogalvanic effect on the 587.6-nm He transition is presented. Experimental results for the optogalvanic effect on the 587.6-nm He transition are presented. The experimental results and the model agree on the current dependence and on the absolute magnitude of the optogalvanic effect over a factor of 10 in Rp. Substantially more sophisticated models of the positive column are possible, and these positive column models could be used within the mathematical framework of the model of the optogalvanic effect. It should be possible to generalize the model of the optogalvanic effect for other transitions in He, and for other gases. The structure of this model should be useful in determining ionization rates of electronically excited levels from optogalvanic measurements.

ACKNOWLEDGMENTS

I am grateful to Professor A. L. Schawlow and Professor T. W. Hansch for their encouragement and support. I acknowledge helpful discussions with O. D. Judd, S. A. Self, and B. E. Cherrington. This work was supported by the Office of Naval Research under Contract No. ONR N00014-78-0403 and by the National Science Foundation under Grant No. NSF-9687.

APPENDIX

The ionization efficiency for a general two-level system composed of an upper level "u" and a lower level "l" is determined by the rate equations

$$\frac{dn_u}{dt}=0=p_u-n_u\gamma_u-\sigma\left(n_u\frac{g_l}{g_u}-n_l\right)\frac{I}{h\nu} \tag{A1}$$

and

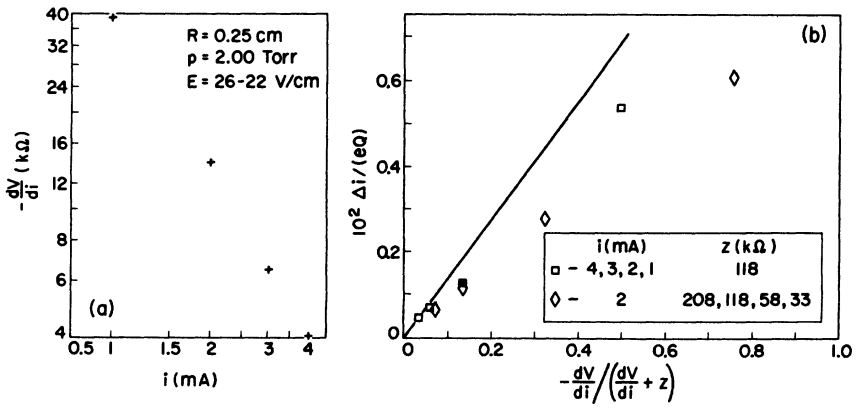

FIG. 6. Dynamic resistance measurements for an Rp of 0.50 cm Torr. (b) Measurements of the magnitude of the optogalvanic effect for an Rp of 0.50 cm Torr.

$$\frac{dn_1}{dt}=0=p_1-n_1\gamma_1+\sigma\left(n_u\frac{g_1}{g_u}-n_1\right)\frac{I}{h\nu}+A\left(n_u-\frac{p_u}{\gamma_u}\right). \quad \text{(A2)}$$

The parameters p_u and p_1 are production terms for the upper and lower level, respectively; γ_u and γ_1 are the sums of the rates of all decay channels for the upper and lower level, respectively; σ is the absorption cross section; g_1/g_u is the ratio of level degeneracies; I is the laser intensity; $h\nu$ is the photon energy; and A is the spontaneous radiative decay rate from u to l. The populations n_u and n_1 have steady-state values p_u/γ_u and p_1/γ_1, respectively, for zero laser intensity. Let γ_1^i be the sum of the rates of all decay channels of the lower level which produce an ion-electron pair directly or indirectly. Let γ_u^i be the sum of the rates of all decay channels of the upper level, except for decay to l, which produce an ion-electron pair directly or indirectly. The ionization efficiency or the number of excess ion-electron pairs produced per absorbed photon is

$$[(n_u-p_u/\gamma_u)\gamma_u^i+(n_1-p_1/\gamma_1)\gamma_1^i]/[(n_1-n_ug_1/g_u)\sigma I/(h\nu)] =\gamma_u^i/\gamma_u-[(\gamma_u-A)/\gamma_u]\gamma_1^i/\gamma_1. \quad \text{(A3)}$$

The right-hand side of (A3) is determined by solving (A1) and (A2) for steady-state values of n_u and n_1 as a function of I and substituting into the left-hand side of (A3). This expression for the ionization efficiency holds for intensities less than, equal to, and greater than the saturation intensity.

[1]R. B. Green, R. A. Keller, G. G. Luther, P. K. Schenck, and J. C. Travis, Appl. Phys. Lett. 29, 727 (1976).
[2]W. R. Bridges, J. Opt. Soc. Am. 68, 352 (1978).
[3]G. C. Turk, J. C. Travis, J. R. Devoe, and T. C. O'Haver, Anal. Chem. 50, 817 (1978).
[4]J. E. Lawler, A. I. Ferguson, J. E. M. Goldsmith, D. J. Jackson, and A. L. Schawlow, Phys. Rev. Lett. 42, 1046 (1979).
[5]J. E. M. Goldsmith, A. I. Ferguson, J. E. Lawler, and A. L. Schawlow, Optics Lett. 4, 230 (1979).
[6]K. C. Smyth, R. A. Keller, and F. F. Crim, Chem. Phys. Lett. 55, 473 (1978).
[7]D. M. Pepper, IEEE J. Quantum Electron. QE-14, 971 (1978).
[8]E. F. Zalewski, R. A. Keller, and R. Engleman, Jr., J. Chem. Phys. 70, 1015 (1979).
[9]R. A. Keller, R. Engleman, Jr., and E. F. Zalewski, J. Opt. Soc. Am. 69, 738 (1979).
[10]R. Deloche, P. Monchicourt, M. Cheret, and F. Lambert, Phys. Rev. A 13, 1140 (1976).
[11]W. L. Wiese, M. W. Smith, and B. M. Glennon, in *Atomic Transition Probabilities*, U. S. National Bureau of Standards Reference Data Series-4 (U. S. GPO, Washington, D. C., 1966), Vol. I, p. 11–14.
[12]H. F. Wellenstein and W. W. Robertson, J. Chem. Phys. 56, 1072 (1972).
[13]H. F. Wellenstein and W. W. Robertson, J. Chem. Phys. 56, 1077 (1972).
[14]W. R. Bennett, Jr., P. J. Kindlmann, and G. N. Mercer, Appl. Opt. Suppl. 2, 34 (1965).
[15]J. C. Gauthier, F. Devos, and J. F. Delpech, Phys. Rev. A 14, 2182 (1976).
[16]J. E. Lawler, J. W. Parker, L. W. Anderson, and W. A. Fitzsimmons, Phys. Rev. Lett. 39, 543 (1977); Phys. Rev. A 19, 156 (1979).
[17]S. Kubota, C. Davies, and T. A. King, J. Phys. B 8, 1220 (1975).
[18]D. Mihalas and M. E. Stoné, Astrophys. J. 151, 293 (1967).
[19]W. Schottky, Phys. Z. 25, 635 (1924).
[20]B. E. Cherrington, IEEE Trans. Electron Devices ED-26, 148 (1979).
[21]L. Tonks and I. Langmuir, Phys. Rev. 34, 876 (1929).
[22]A. D. White and E. I. Gordon, Appl. Phys. Lett. 3, 197 (1963).
[23]P. G. Browne and M. H. Dunn, J. Phys. B 6, 1103 (1973).
[24]P. A. Miller, J. T. Verdeyen, and B. E. Cherrington, Phys. Rev. A 4, 692 (1971); P. A. Miller, Ph.D. thesis, University of Illinois, Urbana (1971) (unpublished).
[25]J. Willison, Stanford University (private communication).
[26]A. V. Phelps, Phys. Rev. 99, 1307 (1955).
[27]D. R. Long and R. Geballe, Phys. Rev. A 1, 260 (1970).
[28]A. V. Phelps and J. R. Molnar, Phys. Rev. 89, 1202 (1953).
[29]R. Mewe, in *Phenomena in Ionized Gases* 1967, Contributed Papers of the Eighth International Conference (Springer, Berlin, 1967), p. 102.
[30]R. J. Bickerton, and A. von Engel, Proc. Phys. Soc. London 69B, 468 (1956).
[31]S. C. Brown, in *Basic Data of Plasma Physics*, 1966 (MIT Press, Cambridge, Massachusetts, 1966), p. 81–82.